Int. J. Nanoelectronics and Materials **10** (2017) 175-184

Modelling and characterization of fabricated metal-insulator-metal capacitors

R. Karthik

Department of Electronics and Communication Engineering, MLR Institute of Technology, Dundigal, Hyderabad – 500043, India

Received 11 Mar 2017; Revised 3 May 2017; Accepted 17 May 2017

Abstract

This paper presents a model for capacitance – voltage characteristics of bilayer metal-insulator-metal capacitors. The proposed model accounts for Space charge and Maxwell-Wagner polarization mechanisms. It is observed that the effective dielectric constant of stack is increased due to the accumulation of charges at the interface of high to low conductance materials due to the applied field. The proposed model for capacitance – voltage characteristics shows a good agreement with experimental results by introducing carrier tunneling probability of dielectric stack. It is observed that the Maxwell Wagner polarization is dominant at low frequencies (<10 KHz). This model indicates that the nonlinearity can be suppressed by choosing the similar permittivity dielectric materials for fabrication of multilayer metal insulator metal capacitors.

Keywords: Anodization, Bilayer, Capacitance – Voltage, Maxwell-Wagner, Metal-Insulator-Metal Capacitor.

1. Introduction

Metal-insulator–metal (MIM) capacitors are attractive passive elements for analog and mixed signal applications. Some sensitive circuits, such as Analog to Digital (A/D) converter Integrated Circuits (ICs), expect a very low variation of capacitance with voltage of less than 100ppm/V^2. In this regard, high-*k* dielectric stack MIM capacitors were proposed by many authors in recent days [1]. It is observed that the voltage coefficient of capacitance (VCC) is higher at low frequencies than at high frequencies. This is due to migration and accumulation of charges at the interface of dielectrics. Such accumulated charges polarize for the applied field; such mechanism is referred as Maxwell-Wagner (MW) polarization [2]

Maxwell - Wagner polarization is observed in many ferroelectric mixtures or heterostructures [3-7]. The accumulation of charges at the interface of heterostructures for the applied field leads to enhancement of effective permittivity [5]. A giant dielectric constant of ~1000 was achieved with ALD TiO_2/Al_2O_3 nanolaminates by Wei Li *et al* [8]. Because of MW polarization, the each TiO_2/Al_2O_3 interface accumulation yields a high dielectric constant of 750 times greater than that of Al_2O_3. Recently, MW effect was found

*)For Correspondence. E-mail: rayam16@gmail.com

in MOS device by Jinesh *et al* [9]. It is worth to note that the MW charge accumulation is observed in forward bias only, i.e., the charge injection from high conductive to low conductive high-*k* material [10]. The approach of imaginary permittivity ε" to ∞ in forward bias at low frequencies indicates the presence of MW polarization [9]. However, models developed in these reports have ignored the dependence of applied potential across the dielectric stack.

Many reports are available on the modeling of dependence of capacitance with voltage for single layer dielectric MIM capacitors [10]. However, to the best of our knowledge, the modeling of capacitance-voltage characteristics of bilayer or multilayer MIM capacitors is not reported yet. In this paper, we have developed a model for voltage dependence of bilayer dielectrics MIM capacitor using MW polarization. This model accounts the carrier tunneling probability of dielectric stack and MW relaxation time of accumulated interfacial charges. A good agreement was found between the model and the measured capacitance-voltage characteristics of TiO_2/Al_2O_3 MIM capacitors. It is observed that the MW polarization is significant in low frequencies of <10 KHz.

2. Experimental Procedure

A 100nm SiO_2 was grown by dry oxidation at a temperature of 1100^oC at about 30 minutes on Si substrate and thoroughly cleaned by deionized water. Over that, a bilayer of 15nm Ti on 100nm Al is deposited using electron beam evaporator with tungsten filament at a pressure of 8×10^{-5}mBar. This Ti/Al film was anodized potentiostatically using non-aqueous solution of ammonium pentaborate dissolved in ethylene glycol ($20gl^{-1}$) by the same size of platinum cathode. Oxidation was done for various anodization voltages of 25V (Sample 1) and 30V (Sample 2) until the anodization current density reduces to $1\mu A/cm^2$. Only three-quarters of sample area were dipped in the electrolyte to avoid etching for bottom electrode. This forms a barrier type anodic bilayer TiO_2/Al_2O_3 at lower and higher anodization voltages, respectively. After cleaning thoroughly by deionized water, a 50nm thick Al top electrode was deposited on the samples using thermal evaporation with the shadow mask area of ~$0.61mm^2$. Samples 1 and 2 are bilayer TiO_2/Al_2O_3 MIM capacitors. SEM cross-sections of the samples 1 and 2 are shown in Figure 1. Due to the delamination of TiO_2 from bottom Al_2O_3 at higher anodization voltages, the anodization voltage was restricted to 30V (> 30V, not shown).

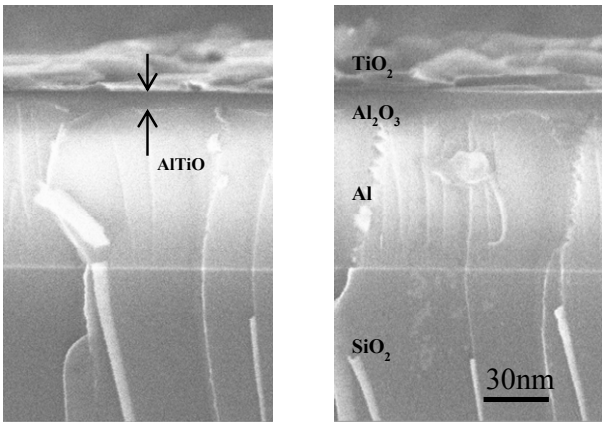

Fig. 1: SEM cross section image of anodized region before top electrode deposition (a) Sample 1 (AV=25V) (b) Sample 2 (AV=30V)

Fig. 2 shows the depth profile of the two samples using secondary ion mass spectrometry (SIMS) in positive mode with 1kVCs. 30kV gallium ion was used as the primary ion during the SIMS measurement**.** It shows ion distribution of Ti, Al, O, Si, Ti-O and Al-O. It is observed that the inward migration of oxygen ion increases, which forms a thin layer of Al_2O_3. It is also observed that outward migration of Al into TiO_2 is increased, which increases the thickness of AlTiO composite layer.

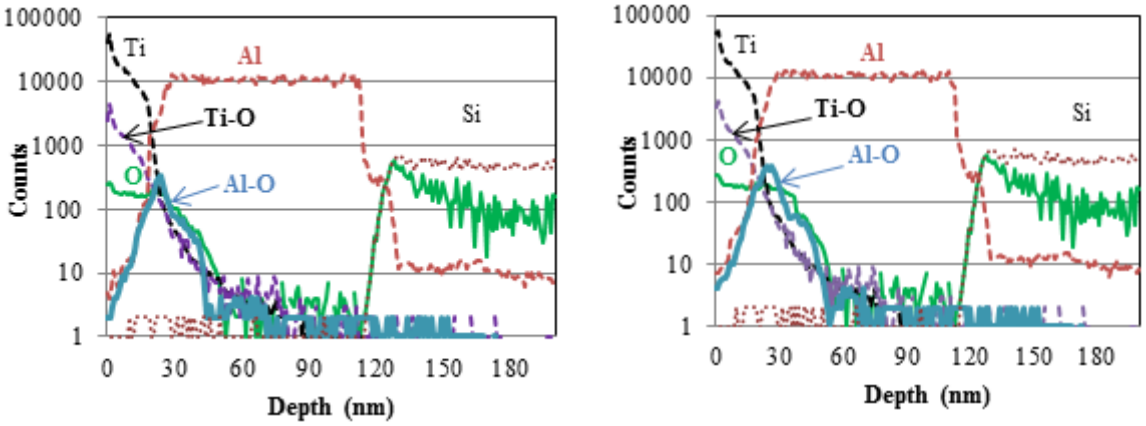

Fig. 2. SIMS depth profile of all samples (a) Sample 1 (b) Sample 2

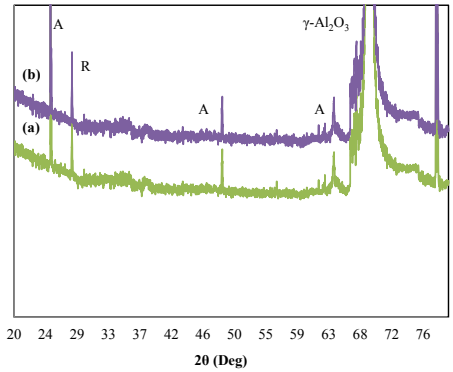

Fig. 3. X-Ray diffraction spectra of anodized samples at various anodization voltages (a) 25V (b) 30V (A: Anatase, R: Rutile)

Fig. 3 shows the X-ray diffraction patterns of the anodized samples. It is observed that the crystalline phases of TiO_2 anatase and rutile are present at all anodization voltages. Also, the crystalline Al_2O_3 (γ-Al_2O_3) emerges at $2\theta=65.5^o$ for both the samples. The migration of oxygen and evolution of electrons into Al region increases and forms bilayer TiO_2/Al_2O_3 with a thin layer of crystalline Al_2O_3 near TiO_2/Al_2O_3 interface [10].

The capacitance and leakage current density were measured using semiconductor parameter analyzer (HP4155C). The measured leakage current density as a function of applied voltage for all the samples is reported in our earlier work [11]. It has been observed that most of the samples are showing high degree of asymmetry at forward and reverse biases and leakage current of Sample 1 and Sample 2 drastically reduces. These are due to formation of AlTiO interfacial layer and TiO_2/Al_2O_3 stack. A detailed discussion of leakage characteristics and conduction mechanism of this bilayer MIM capacitors are reported in [11].

3. Results and Discussion

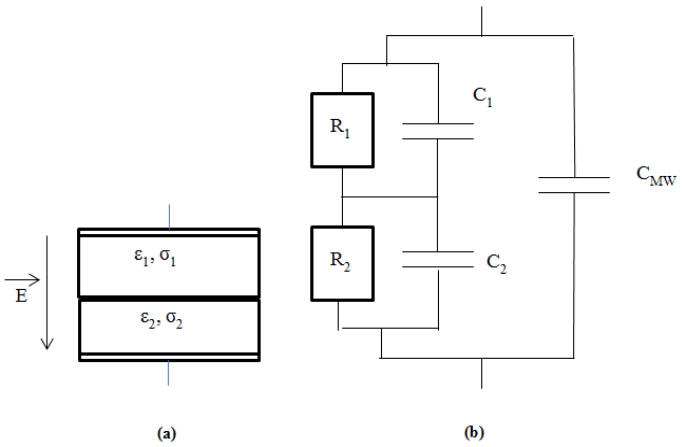

Fig. 4: Schematic of bilayer configuration (a) Layer specification, (b) Equivalent circuit at low frequencies.

Consider a bilayer MIM structure as shown in Fig. 4 (a). The layers consist of two dielectric materials with distinct relative dielectric constant of ε_{r1} and ε_{r2} with thickness of d1 and d2, respectively. Each layer's conductivity and relaxation time are represented as σ_n and τ_n, respectively, for n =1, 2. Fig. 4 (b) shows the equivalent RC network of bilayer MIM structure. Here R1 & C1 and R2 & C2 are individual resistance & capacitance of layer-1 and layer-2, respectively. C_{MW} is interfacial capacitance, also called "Maxwell-Wagner capacitance", which is significant at low frequencies. To calculate the charge density of dielectric interface, Maxwell's time varying accumulation process at pure insulator interface is considered. This charge density is used to calculate the interfacial capacitance, named as C_{MW}. The values of R_1 and R_2 are ignored to calculate the total capacitance value due to their high values. The total capacitance can be expressed as,

$$C_{total}(V_B) = \left(\frac{1}{C_1} + \frac{1}{C_2}\right)^{-1} + C_{MW}(V_B) \tag{1}$$

where MW capacitance can be calculated by $C_{MW} = A.\ q^2.N_{MW}$ where q is charge of an electron and A is top electrode area of capacitor [12]. According to MW theory of double layer [12-13], the accumulated charge density at the interface as a function of applied potential and time is expressed as [14],

$$N_{MW} = \varepsilon_0 \left[\frac{\varepsilon_1\sigma_2 - \varepsilon_2\sigma_1}{d_1\sigma_2 + d_2\sigma_1}\right].V_{stack}\left(1 - e^{\left[-t/\tau_{MW}\right]}\right) \tag{2}$$

Here V_{stack} is voltage across the bilayer dielectric stack for the applied bias voltage V_B; t is time of measurement and τ_{MW} is relaxation time of double layer. The accumulated interface charges and native traps build up potential, which opposes the applied field and reduces flow of charges, so the potential across stack can be written as $V_{stack} = |V_B - V_{bi}|$ where V_{bi} is built in potential at interface due to accumulated interface charges. This MW time constant (τ_{MW}) of double layer can be expressed as,

$$\tau_{MW} = \frac{\left(\varepsilon_2 d_1 + \varepsilon_1 d_2\right)}{\left(d_1\sigma_2 + d_2\sigma_1\right)} \tag{3}$$

If the measurement time *t* is greater than τ_{MW}, then the third term of Eq. (2) can be eliminated. Therefore, the Eq. (2) can be rewritten as,

$$N_{MW} = \varepsilon_o\left[\frac{\left(\varepsilon_{r1}\sigma_2 - \varepsilon_{r2}\sigma_1\right)}{d_2\sigma_1 + d_1\sigma_2}\right].\left|V_B - V_{bi}\right| \tag{4}$$

We know, $\tau_1 = \frac{\varepsilon_1}{\sigma_1}$ & $\tau_2 = \frac{\varepsilon_2}{\sigma_2}$ and $G_1 = \frac{\sigma_1}{d_1}$ & $G_2 = \frac{\sigma_2}{d_2}$. By substituting these in Eq. 4,

$$N_{MW} = \frac{G_1 G_2}{G_1 + G_2}\left[\tau_1 - \tau_2\right].\left|V_B - V_{bi}\right| \tag{5}$$

G_1, G_2, τ_1, τ_2 are defined as the conductance and relaxation time of layer 1 and layer 2. Here $\frac{G_1 G_2}{G_1 + G_2} = G$, where G is the total conductance of bilayer. Therefore, Eq. (5) can be reduced to,

$$N_{MW} = G\left[\tau_1 - \tau_2\right].\left|V_B - V_{bi}\right| \tag{6}$$

The total conductance G is a frequency sensitive term. It is expresses as $G = \omega C_0 \varepsilon''$,where C_0 is the capacitance at zero bias, ε'' is imaginary part of dielectric permittivity. $\varepsilon''$of bilayer dielectric stack can be expressed as [5],

$$\varepsilon'' = \frac{1 + \omega^2\left[\left(\tau_{MW}.\tau_1\right) + \left(\tau_{MW}.\tau_2\right) - \left(\tau_1.\tau_2\right)\right]}{\omega C_0\left(R_1 + R_2\right)\left[1 + \omega^2\tau_{MW}^2\right]} \tag{7}$$

Thus Eq. 5 becomes,

$$N_{MW} = \frac{1 + \omega^2\left[\left(\tau_{MW}.\tau_1\right) + \left(\tau_{MW}.\tau_2\right) - \left(\tau_1.\tau_2\right)\right]}{\left(R_1 + R_2\right)\left[1 + \omega^2\tau_{MW}^2\right]}\left[\tau_1 - \tau_2\right].\left|V_B - V_{bi}\right| \tag{8}$$

The compatibility of proposed model with measured capacitance for the applied voltages at various frequencies are shown in Fig. 5 (a) and 5 (b) for samples 1 and 2, respectively. Table 1 shows the parameters adopted for fitting this model with measured capacitance. Since the Eq. 8 has linear relation of applied voltage with accumulated charge density, it does not fit with measured C-V characteristics. This is due to the ignorance of charge migration between dielectric materials. According to Maxwell and Wagner, the dielectric layers are thick and pure insulators, which do not conduct. But the fabricated bilayer nanostructured thin films have sufficiently large conductivity. The migration of charges for the applied potential can be incorporated to Eq. (8).

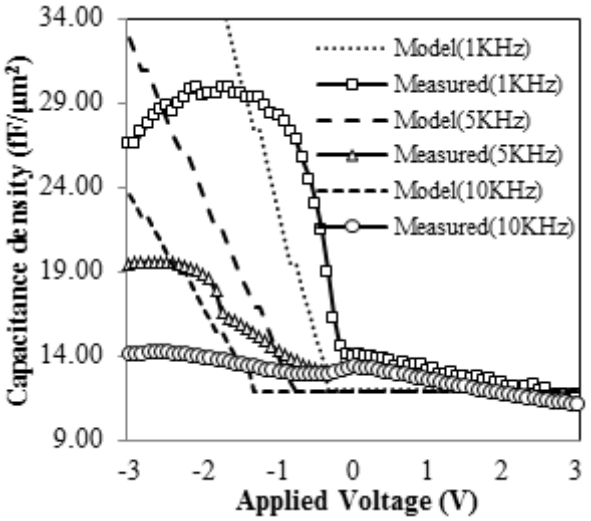

(a)

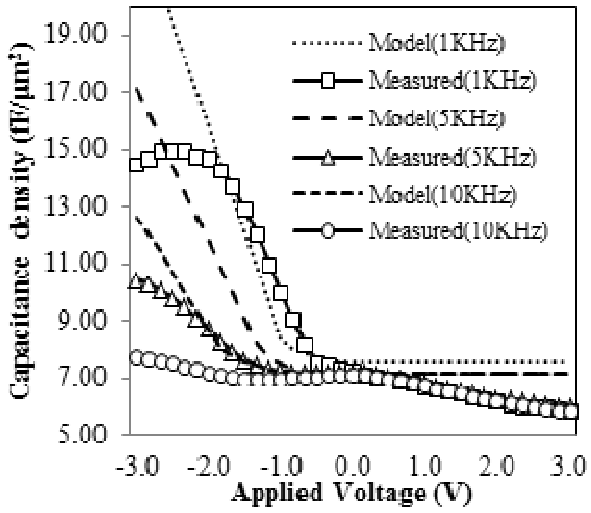

(b)

Fig. 5: MW C-V Model (without tunneling probability) and Measured C-V fitting compatibility for samples (a) Sample 1, (b) Sample 2

Table 1: Fitting Parameters of Maxwell-Wagner Capacitance Model

Sample name	d1 (nm)	d2 (nm)	ε_{r1}	ε_{r2}	σ_1 (pS/ cm)	σ_2 (pS/cm)	Φ_1 (eV)	Φ_2 (eV)	V_{bi} (eV)
Sample 1	15	7	90	9	15	2×10^{-3}	3.3	2.3	1
Sample 2	15	10	90	9	15	4×10^{-3}	3.3	2.3	1.2

To incorporate this realistic situation, tunneling probability has been added using trap assisted tunneling model [15-16]. Therefore Eq. (8) can be rewritten as,

$$N_{MW}(V_b) = q^2 \frac{1+\omega^2((\tau_{MW}.\tau_1)+(\tau_{MW}.\tau_2)-(\tau_1-\tau_2)}{(R_1+R_2)(1+\omega^2\tau_{MW}^2)}.(\tau_1-\tau_2) \quad (9)$$
$$.|(V_b - V_{bi})\{1-\exp[(qV_{stack}-\phi_1+\phi_2+\phi_t-\phi_{ii})/k_BT]\}|$$

where ϕ_1, ϕ_2, ϕ_{ii}, ϕ_t, k_B, and T are the barrier height at Al/TiO_2 interface, barrier height at Al_2O_3/TiO_2 interface, trap barrier height of insulator/insulator interface traps, barrier height of traps, Boltzmann constant and Temperature respectively.

Compatibility of the models are shown in Fig. 6 (a) and 6 (b) along with model with tunneling probability. The proposed model with tunneling probability is showing a better fit with measured data. There is no accumulation of charges present in the forward bias due to which there is no capacitance enhancement. This indicates that model is valid

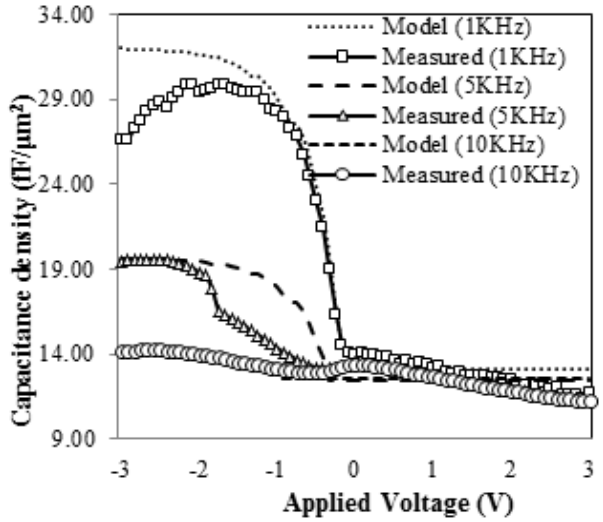

(a)

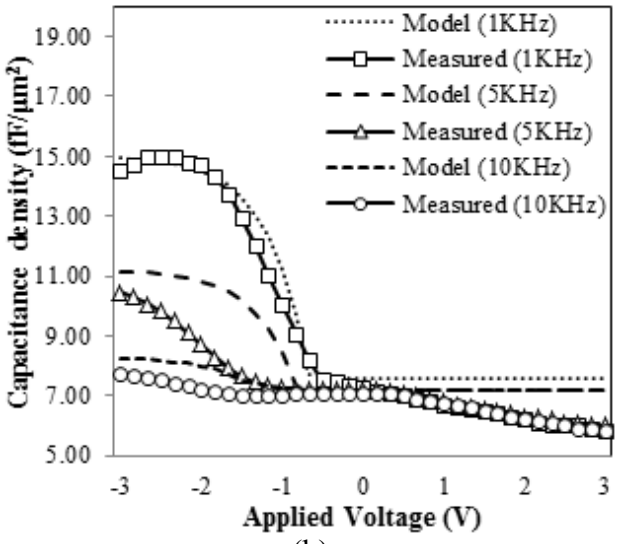

(b)

Fig. 6: MW C-V model (with tunneling probability) and Measured C-V fitting compatibility for samples (a) Sample 1 (10KHz), (b) Sample 2 (1 KHz)

only for reverse bias as the Maxwell Wagner polarization occurs only when the field travels from high to low conductive layer.

MW effect of permittivity enhancement in bilayer MIM capacitors leads to increase in VCC at low frequencies. It is observed that the ratio of permittivity of both dielectric materials determines the MW capacitance. For instance, TiO_2/Al_2O_3 shows a capacitance

enhancement of twice compared to series capacitance of bilayer in our experiments. At the same time, sandwich of TiO_2 and Al_2O_3 multilayer stack shows a giant dielectric constant of > 500 times of single layer MIM structure [8]. Therefore, the dependence of capacitance with voltage can be reduced by choosing the materials with less R_{di}, such as ZrO_2/HfO_2 (29/25=1.6) and HfO_2/Al_2O_3 (29/9=3.22).

4. Conclusion

Capacitance – voltage characteristics of bilayer MIM capacitors are deduced from Maxwell approach on accumulation of charges at dielectric interface. With the Wagner equation on space charge polarization, the voltage dependence of dielectric enhancement is derived. The model shows a good agreement with experiment. It was observed that the Maxwell-Wagner polarization occurs at low frequencies and largely depends on field direction. The charge built-up due to tunneling and accumulation has added more accuracy compared to ideal case. Physics and modeling of capacitance – voltage characteristics of MIM capacitors are useful to analyze the origin of nonlinearities, formation of capacitance, frequency & temperature dependence, and dielectric relaxation in MIM capacitors

Acknowledgement

The authors would like to acknowledge Science and Engineering Research Board, India for financial support.

References

[1] Z X He, D Daley, R Bolam, D Vanslette, F Chen, E Cooney, D Mosher, N Feilchenfeld, K Newton, E Eshun, R Rassel, J Benoit, D Coolbaugh, S S Onge and J Dunn. (2008). IEEE Bipolar/BiCMOS Circ. and Tech. Meet., 212
[2] Sillars R W. (1937). J. of the Inst. of Elect. Eng., 378
[3] G E Shui Bing, Shen Ming Rong, Ning Zhao Yuan, Chin. (1996). Phy. Lett., **19**, 563
[4] Qu B D, M Evstigneev, D J Johnson and R H Prince. (1998). Appl. Phy. Lett. 1394
[5] O'Neill D, R M Bowman and J M Gregg. (2000). Appl. Phy. Lett., **77**, 1520
[6] G Catalan, D O'Neill, R M Bowman, J M Gregg. (2000). Appl. Phy. Lett., **77**, 3078
[7] M Shen, S Ge, W Cao. (2001). J. of Phy. D: Appl. Phy., **34**, 2935
[8] Li W, O Auciello , R N Premnath, B Kabius. (2010). Appl. Phy. Lett., **96**, 162907
[9] K B Jinesh , Y Lamy, J H Klootwijk, W F A Besling. (2009). Appl. Phy. Lett., **95**, 122903
[10] R Karthik, D Kannadassan, Maryam Shojaei Baghini, P S Mallick. (2013). J. of Nanosci. & Nanotech., **13**, 1
[11] D Kannadassan, R Karthik, Maryam Shojaei Baghini, P S Mallick. (2014). Sol. Stat. Electron., **91**, 112
[12] S M Sze, K Ng Kwok. (2006). Physics of Semiconductor Devices, John Wiley & Sons
[13] Maxwell, James clerk, A treatise on electricity and magnetism, Oxford: Clarendon Press (1873)
[14] P H F Morshuis, R Bodega, D Fabiani, G Montanari, L A Dissado, J Smit, IEEE Intern. Conf. on Sol. Dielec., ICSD, (2007) 450
[15] M Houssa , M Tuominen, M Naili, V Afanas'ev, A Stesmans, S Haukka, M M Heyns, J. of Appl. Phys., 87 (2000) 8615

[16] Hassan, M.A.M., Al-Kadhemy, M.F.H., Salem, E.T., Int. J. of Nanoelectron. and Mat., 8 (2015) 69